Journal of Materials Chemistry C

ROYAL SOCIETY OF CHEMISTRY

PAPER

Cite this: J. Mater. Chem. C, 2025, 13, 842

Pi-extended hypervalent iodine macrocycles and their supramolecular assembly with Buckminsterfullerene†

Krishna Pandey, Samsul Arafin, Grayson Venus, Eli Jones, Yachu Du, Mina Dumre Pandey, Tahir Awais, Lichang Wang and Kyle N. Plunkett *

Received 3rd October 2024,
Accepted 4th November 2024

DOI: 10.1039/d4tc04251d

rsc.li/materials-c

A series of valine functionalized supramolecular hypervalent iodine macrocycles (HIMs) with enlarged aromatic cores, including naphthalene and anthraquinone, have been synthesized. Single crystal analysis shows the macrocycles consist of a slightly distorted cyclic planner interior with three carbonyl oxygens from the amino acid residues facing towards the center of the macrocycle and all three alkyl groups above one plane. Owing to the enlarged aromatic core, the naphthalene-based HIMs were successfully co-crystallized with Buckminsterfullerene (C_{60}) into a long-range columnar supramolecular structure. The assembled architecture displays a long-range pattern between HIM and C_{60} in a 2 : 3 ratio, respectively. Disassembly of the HIMs can be accomplished by adding anions of tetrabutylammonium (TBA) salts that selectively bind with the electron deficient iodine center in HIM systems. A comparative study of the associations constants and the binding energies for different aromatic-based HIMs with TBA(Cl) and TBA(Br) is presented.

Introduction

Supramolecular chemistry involves molecular recognition through noncovalent interactions in small molecules that enable self-assembly into higher order structures for a broad range of applications in physical and biological sciences.[1] Self-assembly is often mediated by weak non-covalent intermolecular forces such as hydrogen bonding, metal coordination, hydrophobic forces, van der Waals forces, pi–pi interactions, and electrostatic effects.[2,3] As an alternative, the additional intermolecular hypervalent interactions known as secondary bonding, could contribute to new classes of stable supramolecular structures.[4] Secondary bonding shares structural features with hydrogen bonding and this bonding plays a paramount role in the self-assembly of monomers into intricate supramolecular architectures based on hypervalent iodine.[5–7] Our research is interested in harnessing hypervalent iodine's secondary bonding as an alternative to conventional non-covalent interactions for the synthesis of higher order supramolecular assemblies.

The term ''hypervalency'' is defined as the ability of an atom to expand its valence shell beyond the limits of the Lewis octet rule.[8] Among several atoms capable of hypervalency, hypervalent iodine-based molecules are the most widely studied due to their unique reactivities, low toxicity, high stability, ease of handling, and economical advantages over heavy metal reagents.[9,10] Secondary bonding is characterized as those interactions that involve intermolecular hypervalent connections with lengths shorter than the sum of the van der Waals radii between a heavy p-block element and an electron pair donor (typically O, N, S, or halogen).[11]

One variation of hypervalent iodine exists as λ^3-iodanes where the iodine atom contains a total of 10 electrons, classifying them under the 10-I-3 nomenclature as shown in Fig. 1. These compounds exhibit a distorted trigonal bipyramidal geometry, with two heteroatom ligands (X) positioned at the apical positions, while the least electronegative carbon ligand (R) and both electron pairs are situated equatorially. This configuration results in a distinct T-shaped geometry, crucial for stabilizing hypervalent iodine systems.[12] The two X ligands are linearly attached to a single 5p orbital, forming a 3-center-4-electron (3c–4e) bond system.[13–15] In this arrangement, the bond length of one heteroatom with the iodine is influenced by the bond strength of the other heteroatom.[16]

Various studies[6,7,16,17] have highlighted the use of secondary bonding interactions (a fourth association at the iodine center) between iodine and oxygen in the development of hypervalent iodine-based materials. In 1991, Ochiai[17] synthesized the first supramolecular structure of this kind, a macrocycle derived from 1-alkynyl-1,2-benziodoxol(1*H*)-ones (Fig. 1), demonstrating the importance of secondary bonds between hypervalent iodine and adjacent carbonyl oxygen facilitating the assembly

School of Chemical and Biomolecular Sciences, Southern Illinois University, Carbondale, IL 62901, USA. E-mail: kplunkett@chem.siu.edu

† Electronic supplementary information (ESI) available: Detailed experimental procedures, NMR spectra, X-ray crystallography details. CCDC 2388281–2388283. For ESI and crystallographic data in CIF or other electronic format see DOI: https://doi.org/10.1039/d4tc04251d

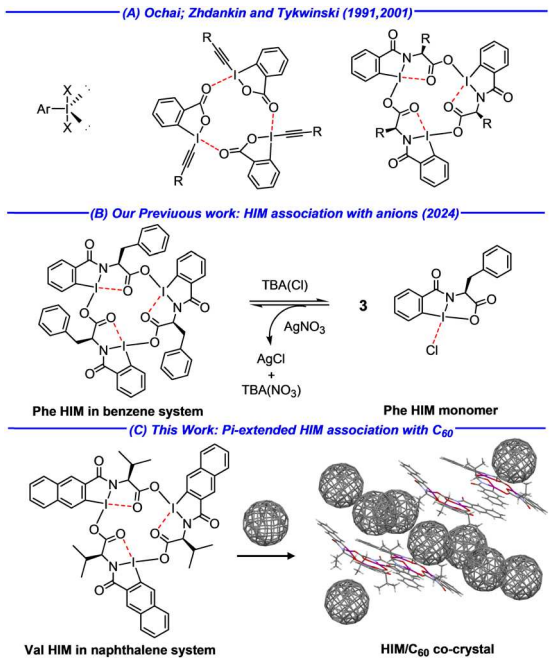

Fig. 1 (A) "T" shaped bonding in λ^3-iodanes (left), Selected previous examples of HIMs: Ochai; 1991 (middle), Zhdankin and Tykwinski; 2001 (right). (B) Our previous work: assembly and disassembly of HIMs through anion coordination. (C) This work: supramolecular assembly of pi extended HIMs and their assembly with Buckminsterfullerene.

of monomer into a trimeric structure. This concept was furthered in 2001 by Zhdankin and Tykwinski[6] where amino-acid based hypervalent iodine macrocycles (HIMs) were prepared *via* the self-assembly of three oxidized benziodazoles (Fig. 1) to give a hypervalent iodine macrocycle (HIM). This discovery highlights the significance of secondary bonding interactions in the synthesis of HIM-based supramolecular architectures.

In previous work[18] (Fig. 1B), analogs of HIMs were synthesized and their dynamic nature in solution was demonstrated through the reversable disassembly and re-assembly by addition or removal of anions such as chloride, bromide, fluoride and cyanide, respectively. Furthermore, it was found that the HIMs are dynamic in the absence of additional anions and HIM monomers can exchange with other macrocycles to participate in dynamic covalent chemistry based on secondary bonding in these systems.

In this contribution (Fig. 1C), it was found that larger aromatic cores in the HIM systems enable additional supramolecular assemblies involving pi-stacking. HIMs with larger aromatic cores including naphthalene and anthraquinone were prepared. This study explores that naphthalene-based HIMs co-assemble with C_{60}, forming ordered crystals with a HIM : C_{60} ratio of 2 : 3, which is enabled by pi–pi interactions between the two species and leads to long range order. Lastly, we have experimentally and computationally compared the association constants of tetrabutylammonium anion salts with the hypervalent iodine center in the three different HIMs systems. An initial version of this work was deposited in ChemRxiv on October 3, 2024.[19]

Results and discussion

The synthesis of the new HIM systems followed a similar procedure to our previous work with benzene based HIMs **6a** (Scheme 1).[6,18] Starting materials based on naphthalene **1b** and anthraquinone **1c** were synthesized *via* previously developed protocols.[20,21] The HIM precursors were then synthesized by combining **1a–c** with the commercially available L-valine tertiary butyl ester hydrochloride **2** *via* a EDC-HCl and HOBt based amide coupling reaction to give intermediates **3a–c** in good yields. These intermediates were deprotected with trifluoracetic acid to give HIM precursors **4a–c**. The synthesis of the final HIMs with benzene (**6a**), naphthalene (**6b**), and anthraquinone (**6c**) were accomplished by oxidation of intermediates **4a–c** with 3-chloroperbenzoic acid (Scheme 1). The final HIM macrocycles are obtained following a rearrangement on the secondary bonds of intermediate macrocycles **5a–c**. The final HIM structures were fully characterized by ^{1}H and ^{13}C NMR spectroscopy and high-resolution mass spectrometry (HRMS). In addition, the structure of the new valine-based naphthalene HIM **6b** was further confirmed by single crystal x-ray diffraction analysis (Fig. 2). The single crystal of **6b** suitable for X-ray crystallography was obtained by vapor diffusion of diethyl ether into a chloroform solution of **6b**. Analogous to the previously reported single crystal structure of valine HIM **6a**,[18] the resulting crystal structure reveals that **6b** is a distorted planner macrocyclic system with the amino acids carbonyl oxygens facing inside the ring. All three isopropyl groups are located above a single plane (Fig. 2).

To compare the photophysical properties of HIMs based on benzene **6a**, naphthalene **6b** and anthraquinone **6c** systems, solution-based UV-vis spectroscopy and fluorescence spectroscopy were used. The solution-based UV-vis spectra of the HIMs (**6a–c**) are shown Fig. 3. As expected, an overall red-shift is observed upon enlarging the aromatic core from benzene to naphthalene to anthraquinone. A sharp high energy absorption band centered at ~240 nm is observed for all three HIMs. HIM **6c** is most red shifted with onset of absorption at 390 nm, while the longest wavelength absorptions of **6a** and **6b** were 365 nm and 351 nm, respectively. Solutions of the HIM compounds showed no discernable fluorescence properties (Fig. S14, ESI†) and is most likely owing to the heavy atom effect of the iodine.

The notable assembly between different classes of supramolecular macrocycles with fullerenes such as C_{60} and C_{70} is well documented.[22–27] Research into the organization of supramolecular assemblies with fullerenes is rapidly emerging and hold promise for applications in sensing,[28] chemical separation,[29] organic electronics,[30] photovoltaics,[31] semiconductors,[32] and light energy harvesting devices[33] to name few. Because of these surprising applications in material sciences, C_{60} is becoming a special guest for several supramolecular hosts. While most of the supramolecular hosts for fullerene are assembled through traditional non-covalent interactions, self-assembly of fullerene with HIMs based on secondary bonding could be another approach to investigate the supramolecular host guest chemistry for material science applications. Therefore, C_{60} was chosen for this study

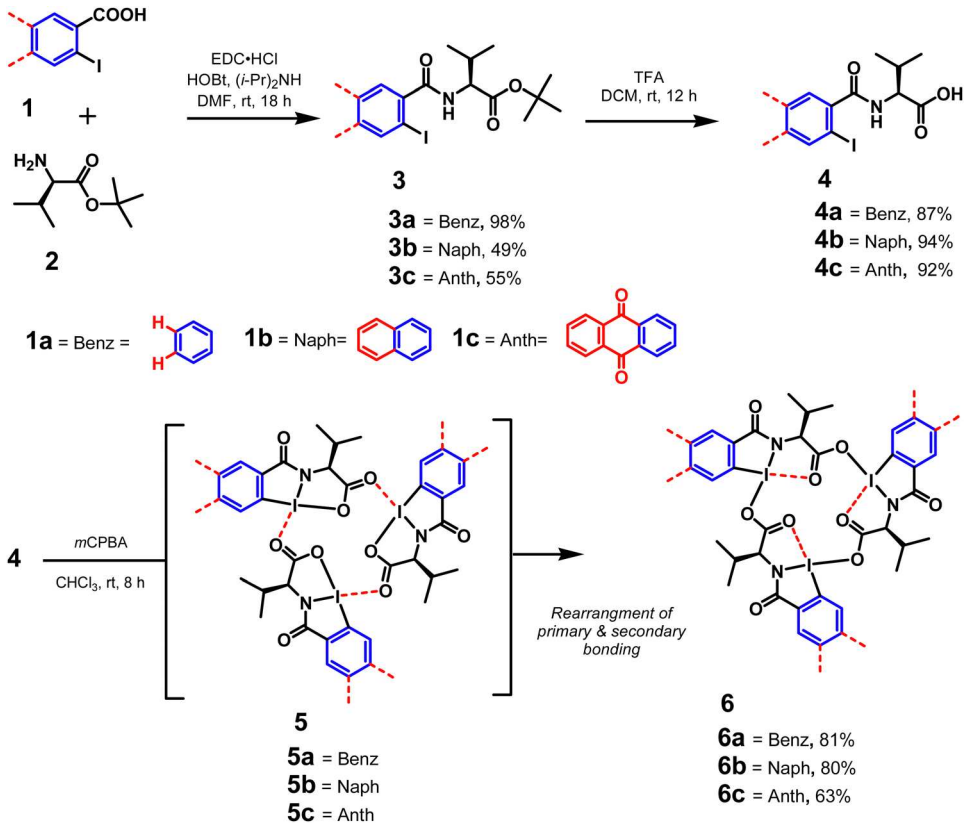

Scheme 1 Synthesis of amino acid based hypervalent iodine macrocycle in naphthalene and anthraquinone system[a]. [a] Rearrangement of secondary bonding gives the more stable "*T*" binding motif around hypervalent iodine leads to a stabilized macrocycle.

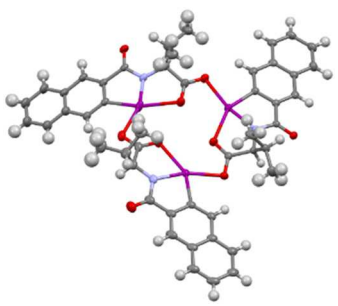

Fig. 2 Crystal structure of HIM **6b**. Thermal ellipsoids drawn at 50% probablity.

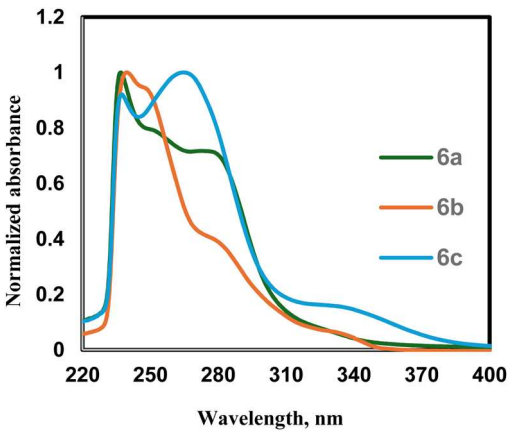

Fig. 3 Absorbance spectra of HIM **6a–6c** (3.6 μM in chloroform).

owing to its ability to form π–π stacking with π-extended aromatics to form new supramolecular architecture and ease of crystal growth. We hypothesized that introducing larger conjugated systems such as naphthalene and anthracene into HIM framework could provide an opportunity for self-assembly with fullerenes such as C_{60} *via* π–π interactions.

First, the co-assembly of HIMs with C_{60} was investigated through NMR titrations. The NMR data (Fig. S1, ESI†), demonstrated that an excess of C_{60} led to a small downfield shift for one of the aromatic singlets. Similar shifting was also noticed for the valine methyl peak within the aliphatic region. While the signal shifts were small, they did suggest some association in solution between the two species. Multiple crystallographic experiments were conducted with a saturated solution of C_{60} and various HIMs using a series of solvents *via* both slow evaporation and vapor diffusion methods. However, attempts to grow co-crystals of HIM **6a** with C_{60} were unsuccessful, resulting instead in well-diffracting crystals of a C_{60} diethyl ether solvate.[34] However, large dark red crystals were obtained from the co-crystallization of **6b** and C_{60}. The molecular structure of these crystals, grown from a chloroform and

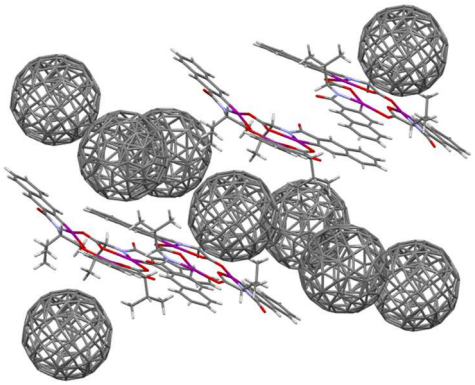

Fig. 4 Crystal packing of **6b**/C_{60} complex resulted from π–π interactions between aromatic residue of HIM and fullerene.

1,2-dichlorobenzene mixture with vapor diffusion of diethyl ether, revealed the formation of an interdigitated supramolecular complex between the **6b** and C_{60} (Fig. 4).

The **6b**/C_{60} crystalized in monoclinic crystal system with space group $P2_1$. The new supramolecular crystal structure comprises of **6b** and C_{60} in a 2 : 3 ratio, wherein **6b** and C_{60} organize into a repeating pattern of FHHFHHF (F = fullerene and H = HIM) as shown in Fig. 5. This complex also demonstrates a host–guest interaction, with the HIMs serving as the host molecule, accommodating multiple fullerene C_{60} guest molecules in an organized fashion. The main driving forces governing this assembly are intermolecular π–π interactions, particularly between naphthalene-naphthalene and naphthalene-fullerene pairs. It is noteworthy that the crystal packing of the co-crystal of HIM **6b** and fullerene in a 2 : 3 ratio reveals prominent π-stacking interactions between two naphthalene units (Fig. S2, ESI†), with specific stacking distances observed at 3.409 Å for C11–C27 and 3.332 Å for

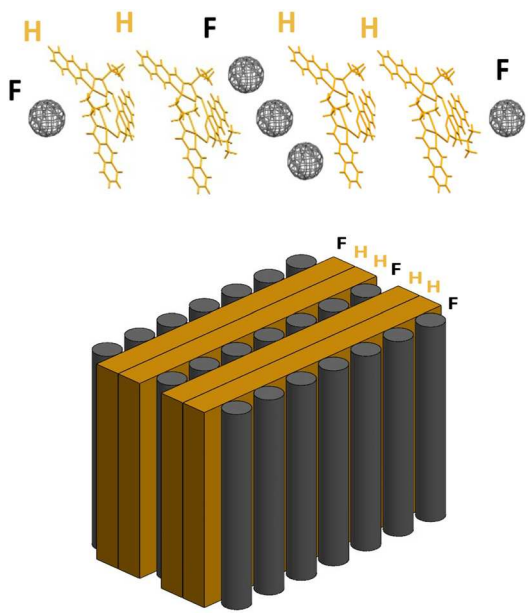

Fig. 5 Organization of HIM and C_{60} in co-crystalline complex Top) general packing arrangement, bottom) 3D representation.

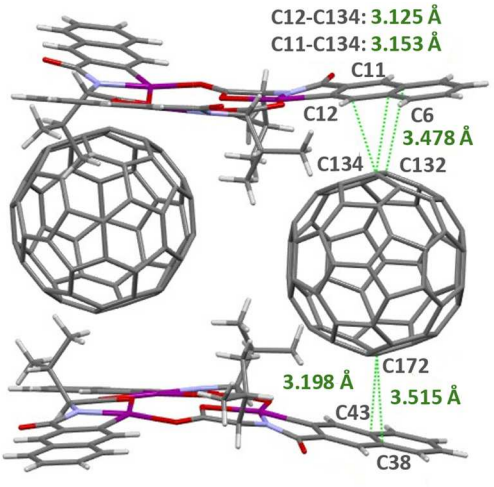

Fig. 6 Crystal structure of complex showing π–π stacking between naphthalene and C_{60}.

C12–C22. (Table S1, ESI†). Furthermore, the π–π stacking interactions between HIM **6b** and C_{60} is substantiated by robust interactions between the naphthalene moiety and fullerene (Fig. 6 and Table 1). Notably, the stacking distances of 3.125 Å between C12–C134 and 3.153 Å between C11–C134 (Table 1) highlight these strong π–π stacking bonds. The other π–π stacking interactions between carbon atoms of naphthalene and fullerene are listed in Table 1 and range from 3.125 Å to 3.515 Å.[35–38] Additional details on the π–π stacking interactions between naphthalene-fullerene pairs are provided in the ESI† (Fig. S3). Previously, it has been demonstrated **6a** could reversibly bind anions that led to the disassembly of the macrocyclic structures. As a comparison, we analyzed anion binding in the new larger **6b** and **6c**. The ability of the HIM **6b** and **6c** to bind certain anions were assessed by means of an ^{1}H NMR titration with tetrabutylammonium chloride TBA(Cl) in $CDCl_3$. (Fig. 7, additional data points are provided in ESI†). In the titration spectra of HIM **6b** with TBA(Cl), significant spectral changes are observed where aromatic protons of HIM **6b** (*d*–*i*) transformed into a new set of signals (*d*'–*i*'). The original protons associated with HIM **6b** were no longer visible in the spectra upon the addition of approximately 1.8 equivalents of TBA(Cl). A similar trend was identified in the NMR titration experiment of **6b** with TBA(Br). It is noteworthy that the emergence of the new species occurred with the addition of approximately 0.9 equivalents of

Table 1 Pi–Pi stacking distances between HIM **6b**- and C_{60}

Carbon atoms	Pi–Pi stacking distance (Å)
C11–C134	3.153
C6–C132	3.478
C12–C134	3.125
C43–C172	3.198
C38–C172	3.515
C22–C110	3.426
C28–C114	3.171
C22–C65	3.378
C27–C65	3.320

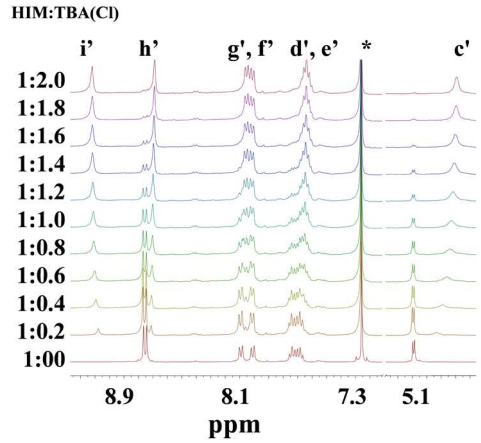

Fig. 7 ^{1}H NMR (400 MHz, 298 K) titration of **6b** with TBA(Cl) at an incremental equivalency in $CDCl_3$. Proton assignments found in Fig. 8.

TBA(Cl) for HIM **6a**,[18] whereas for HIM **6b**, this transformation was observed with considerably more TBA(Cl) (1.8 equivalents). Similar to what was seen in HIM **6a** and **6b**, HIM **6c** was also able to be completely transformed into the new species with the addition of approximately 1.6 and 4 equivalents of TBA(Cl) and TBA(Br), respectively (Fig. S8 and S9, ESI†). Analogous to our previous report,[18] a monomeric species (**6b-adduct**) was identified by X-ray crystallography with the chloride ion associated to the electron deficient iodine atom *via* I–Cl bond and one tetraethylammonium cation is present per naphthalene monomer (Fig. 8).

The nature of the I–Cl bond was probed by conducting a reversibility experiment where silver nitrate was added to a HIM **6b**/TBA(Cl) solution. Silver nitrate was found to competitively coordinate the chloride anion forming silver chloride, therefore enabling the monomer to reassemble into the original HIM structures (Fig. 8). This experiment was confirmed by NMR spectroscopy where the addition of silver nitrate to an NMR solution of adduct followed by the removal of the precipitate results in an identical NMR spectrum compared to that of original HIM **6b** prior to the addition of anion. This finding demonstrates all three systems display the same unique type of dynamic equilibrium and reversibility. (Scheme S1 and S2, ESI†).

Binding constants of the monomer anion-complex (H–G) were estimated through NMR titration data. Although the host to guest (TBA salt) ratio can be determined using accurate volumetric measurements, this approach is susceptible to error propagation. Instead, we relied on the integration of the eight α-amino protons of the tetrabutylammonium cation relative to two reference protons from the monomer (fixed concentration). After establishing the H_0/G_0 ratio, the concentration of the H·G complex was determined. To do this, the same reference peak from the TBA analysis integrated and compared to the adduct peak to determine the concentration.

To quantify the associative process of the monomer-anion complex, the NMR titration data were fitted using a 1 : 1 model of monomer to salt (Fig. 9), consistent with the crystallographic evidence confirming the formation of a 1 : 1 H. G complex. Based on these titration data, satisfactory fits were achieved for **6b** and **6c** with both TBA(Cl) and TBA(Br) salts. The association constants corresponding to the binding of the monomer of **6b** with TBA(Cl) and TBA(Br) were calculated to be 617 M^{-1} and 202 M^{-1} respectively. For **6c**, the binding constants with TBA(Cl) and TBA(Br) are found to be 2871 M^{-1} and 770 M^{-1}, respectively. The calculated associations constants for the monomer of **6a** with TBA(Cl) and TBA(Br) were previously found to be 930 M^{-1} and 400 M^{-1}, respectively.[18] These data demonstrate that the anion association is highest for **6c** and lowest for **6b**. The magnitude of the association constant is directly related to the strength of the I–X bond, where X represents the anion directly bonded to iodine.

The variations in association constants of anions with different HIMs monomer (**6a–c**) is attributed with the structural variations in the benzene, naphthalene and the anthraquinone within the HIM framework. DFT calculations were performed to investigate the change in association constants in these systems (Table 2). The relatively high Ka value observed for chloride for **6c** in comparison to HIM monomer **6a** and **6b** is presumed to result from the electron withdrawing inductive effect of two carbonyl groups in anthraquinone that makes the iodine atom more electropositive, consequently increasing the association constants for chloride ion. To gain further insight into the variable binding constants, the binding energies of

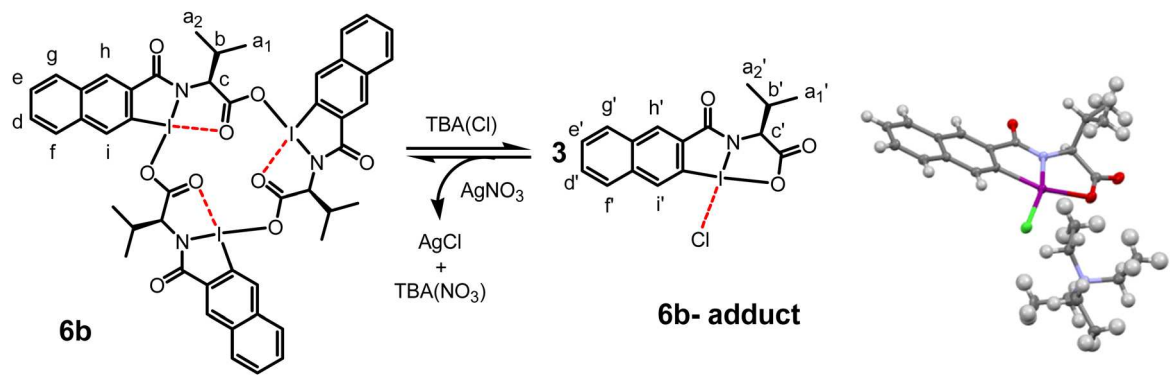

Fig. 8 Left) Scheme of **6b** disassembly and reassembly by addition/removal of chloride anion. The HIM can reform when $AgNO_3$ is added to coordinate the chloride anion. Right) Crystal structure of **6b** adduct showing the I–Cl bond that disrupts the secondary bonding self-assembly in the macrocycle.

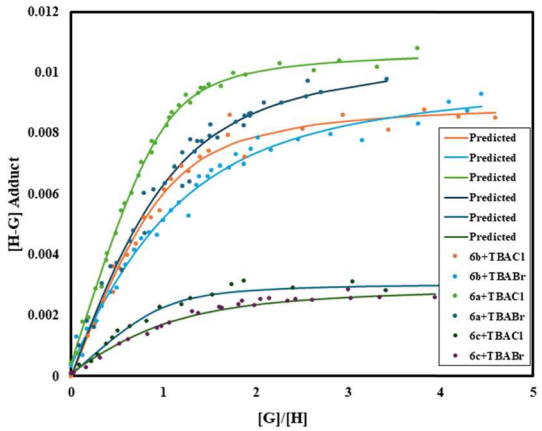

Fig. 9 Isotherms of **6a–c** titrated with TBA(Cl) or TBA(Br). The solid lines are the predicted model fits for each curve. [H] is defined as concentration of monomer (*e.g.*, 3 monomers per HIM).

Table 2 Relative Binding energies and constants of HIM monomer **6a–6c** with chloride and bromide. The details of binding energies and constants are provided in ESI

HIM monomer + TBA(X)	Relative binding energy (KJ mol^{-1})	Charge I (e^{-})	Charge X (e^{-})	Binding constant (M^{-1})[a]
6a-Cl	+4	1.073	−0.707	900
6b-Cl	+4.6	1.074	−0.706	617
6c-Cl	0	1.102	−0.689	2871
6a-Br	+4.8	1.044	−0.655	400
6b-Br	+5	1.044	−0.653	202
6c-Br	0	1.073	−0.635	770

[a] The asymptotic error is calculated at the 95% confidence interval level.[39]

different HIM monomers (**6a–6c**) with both chloride and bromide anions were calculated (Table 1). The binding energies were analyzed in terms of relative binding energy assigning 0 KJ mol^{-1} for most stable HIM monomer **6c-Cl** and HIM monomer **6c-Br**. The details of DFT calculations are provided in ESI.† The higher binding constant for chloride for **6c** is supported by observing the **6c-Cl** is more stable than **6b-Cl** and **6a-Cl** by 4.6 KJ mol^{-1} and 4 KJ mol^{-1}, respectively. The calculated charge of the iodine atom and the anion atoms support the general binding constant trends with greater charge found on the iodine for **6c**. Notably, the binding constant magnitude correlated with the strength of the respective I–X bond, where X denotes the anion directly attached to the iodine.

Conclusions

In summary, three variations of HIMs incorporating benzene, naphthalene, and anthraquinone have been synthesized. We report a new supramolecular assembly between **6b** and C_{60} and that the new macrocycles are capable of reversible assembly owing to anion association and dissociation, respectively. Lastly, analysis of the association constants reveals that the HIM aromatic structure can dictate the binding affinity with anions. These results open the avenue for the incorporation of the longer wavelength absorbing conjugated chromophore in the HIM framework. This enhancement will not only improve the photophysical properties but also could enable the rational design of chiral hosts for the molecular recognition and separation of higher fullerene species. Additionally, these data indicate the possibility of HIMs as promising candidates for fabricating ions sensing devices for material science applications.

Author contributions

KP, SA, EJ, YD, MDP, TA, and KNP contributed to synthetic aspects of the work. KP prepared crystals for X-ray analysis. KP and SA performed titration experiments, performed isotherm analysis, and devised the reversibility experiment. GV and LW performed DFT calculations. KNP envisioned the experimental direction of the project. KP and KNP wrote the manuscript and edited by all authors. All authors have given approval to the final version of the manuscript.

Data availability

The supporting this article have been included as part of the ESI.† In addition, data for three crystal structures were deposited to the CCDC on October 01, 2024 and were assigned numbers 2388281, 2388282, 2388283.†

Conflicts of interest

The authors declare no competing financial interest.

Acknowledgements

We thank the National Science Foundation (CHE-2003654, DMR-2150489), the American Chemical Society Petroleum Research Fund (61467-ND1) and Dr Bob G. and Mrs Beth Gower (Gower Fellowship 2023) for support of this work.

References

1 F. Huang and E. V. Anslyn, Introduction: Supramolecular Chemistry, *Chem. Rev.*, 2015, **115**(15), 6999–7000.
2 D. B. Amabilino, D. K. Smith and J. W. Steed, Supramolecular materials, *Chem. Soc. Rev.*, 2017, **46**(9), 2404–2420.
3 J. L. Atwood and J. M. Lehn, *Comprehensive supramolecular chemistry*, Pergamon, New York, 1996.
4 J. Starbuck, C. Norman and N. Guy Orpen, Secondary bonding as a potential design element for crystal engineering, *New J. Chem.*, 1999, **23**(10), 969–972.
5 M. Boucher, D. Macikenas, T. Ren and J. D. Protasiewicz, Secondary Bonding as a Force Dictating Structure and Solid-State Aggregation of the Primary Nitrene Sources (Arylsulfonylimino)iodoarenes (ArINSO2Ar'), *J. Am. Chem. Soc.*, 1997, **119**(40), 9366–9376.
6 V. V. Zhdankin, A. E. Koposov, J. T. Smart, R. R. Tykwinski, R. McDonald and A. Morales-Izquierdo, Secondary Bonding-Directed Self-Assembly of Amino Acid Derived Benziodazoles: Synthesis and Structure of Novel Hypervalent Iodine Macrocycles, *J. Am. Chem. Soc.*, 2001, **123**(17), 4095–4096.

7 P. Kiprof and V. Zhdankin, Self-assembly of hypervalent iodine through primary and secondary bonding, *ARKIVOC*, 2003, (vi), 170–178.
8 J. I. Musher, The Chemistry of Hypervalent Molecules, *Angew. Chem., Int. Ed. Engl.*, 1969, **8**(1), 54–68.
9 A. Yoshimura and V. V. Zhdankin, Advances in Synthetic Applications of Hypervalent Iodine Compounds, *Chem. Rev.*, 2016, **116**(5), 3328–3435.
10 P. J. Stang and V. V. Zhdankin, Organic Polyvalent Iodine Compounds, *Chem. Rev.*, 1996, **96**(3), 1123–1178.
11 H. J. Emeléus and A. G. Sharpe, *Advances in Inorganic Chemistry and Radiochemistry*, Academic Press, 1972.
12 M. Ochiai, T. Sueda, K. Miyamoto, P. Kiprof and V. V. Zhdankin, Trans Influences on hypervalent bonding of aryl lambda(3)-iodanes: their stabilities and isodesmic reactions of benziodoxolones and benziodazolones, *Angew. Chem., Int. Ed.*, 2006, **45**(48), 8203–8206.
13 R. E. Rundle, Electron Deficient Compounds, *J. Am. Chem. Soc.*, 1947, **69**(6), 1327–1331.
14 G. C. Pimentel, The Bonding of Trihalide and Bifluoride Ions by the Molecular Orbital Method, *J. Chem. Phys.*, 1951, **19**(4), 446–448.
15 F. Weinhold and C. R. Landis, *Valency and Bonding: A Natural Bond Orbital Donor-Acceptor Perspective*, Cambridge University Press, 2005.
16 P. Kiprof, The nature of iodine oxygen bonds in hypervalent 10-I-3 iodine compounds, *ARKIVOC*, 2004, **2005**(4), 19–25.
17 M. Ochiai, Y. Masaki and M. Shiro, Synthesis and structure of 1-alkynyl-1,2-benziodoxol-3(1*H*)-ones, *J. Org. Chem.*, 1991, **56**(19), 5511–5513.
18 K. Pandey, S. Arafin, E. Jones, Y. Du, G. C. Kulkarni, A. Uddin, T. J. Woods and K. N. Plunkett, Assembly and Disassembly of Supramolecular Hypervalent Iodine Macrocycles via Anion Coordination, *J. Org. Chem.*, 2024, **89**(11), 7437–7445.
19 K. Pandey, S. Arafin, G. Venus, E. Jones, Y. Du, M. D. Pandey, T. Awais, L. Wang and K. Plunkett, *Chemrxiv*, 2024, preprint, DOI: **10.26434/chemrxiv-2024-13rlh**.
20 J. S. A. Ishibashi, J. L. Marshall, A. Mazière, G. J. Lovinger, B. Li, L. N. Zakharov, A. Dargelos, A. Graciaa, A. Chrostowska and S.-Y. Liu, Two BN Isosteres of Anthracene: Synthesis and Characterization, *J. Am. Chem. Soc.*, 2014, **136**(43), 15414–15421.
21 F. C. Whitmore and F. L. Carnahan, The Mercuration Of Anthraquinonedicarboxylic Acids, *J. Am. Chem. Soc.*, 1929, **51**(3), 856–862.
22 X. Chang, Y. Xu and M. von Delius, Recent advances in supramolecular fullerene chemistry, *Chem. Soc. Rev.*, 2024, **53**(1), 47–83.
23 K. Tashiro and T. Aida, Metalloporphyrin hosts for supramolecular chemistry of fullerenes, *Chem. Soc. Rev.*, 2007, **36**(2), 189–197.
24 J. Song, N. Aratani, H. Shinokubo and A. Osuka, A Porphyrin Nanobarrel That Encapsulates C60, *J. Am. Chem. Soc.*, 2010, **132**(46), 16356–16357.
25 D. Canevet, M. Gallego, H. Isla, A. de Juan, E. M. Pérez and N. Martín, Macrocyclic Hosts for Fullerenes: Extreme Changes in Binding Abilities with Small Structural Variations, *J. Am. Chem. Soc.*, 2011, **133**(9), 3184–3190.
26 S. Cui, G. Zhuang, D. Lu, Q. Huang, H. Jia, Y. Wang, S. Yang and P. A. Du, Three-Dimensional Capsule-like Carbon Nanocage as a Segment Model of Capped Zigzag [12,0] Carbon Nanotubes: Synthesis, Characterization, and Complexation with C70, *Angew. Chem., Int. Ed.*, 2018, **57**(30), 9330–9335.
27 W. Meng, B. Breiner, K. Rissanen, J. D. Thoburn, J. K. Clegg and J. R. Nitschke, A Self-Assembled M8L6 Cubic Cage that Selectively Encapsulates Large Aromatic Guests, *Angew. Chem., Int. Ed.*, 2011, **50**(15), 3479–3483.
28 Y. Hashikawa and Y. Murata, Cation recognition on a fullerene-based macrocycle, *Chem. Sci.*, 2020, **11**(46), 12428–12435.
29 W. Brenner, T. K. Ronson and J. R. Nitschke, Separation and Selective Formation of Fullerene Adducts within an MII8L6 Cage, *J. Am. Chem. Soc.*, 2017, **139**(1), 75–78.
30 D. M. Guldi, B. M. Illescas, C. M. Atienza, M. Wielopolski and N. Martín, Fullerene for organic electronics, *Chem. Soc. Rev.*, 2009, **38**(6), 1587–1597.
31 S.-Q. Zhang, Z.-Y. Liu, W.-F. Fu, F. Liu, C.-M. Wang, C.-Q. Sheng, Y.-F. Wang, K. Deng, Q.-D. Zeng, L.-J. Shu, J.-H. Wan, H.-Z. Chen and T. P. Russell, Donor–Acceptor Conjugated Macrocycles: Synthesis and Host–Guest Coassembly with Fullerene toward Photovoltaic Application, *ACS Nano*, 2017, **11**(11), 11701–11713.
32 R. Kaur, S. Sen, M. C. Larsen, L. Tavares, J. Kjelstrup-Hansen, M. Ishida, A. Zieleniewska, V. M. Lynch, S. Bähring, D. M. Guldi, J. L. Sessler and A. Jana, Semiconducting Supramolecular Organic Frameworks Assembled from a Near-Infrared Fluorescent Macrocyclic Probe and Fullerenes, *J. Am. Chem. Soc.*, 2020, **142**(26), 11497–11505.
33 R. Caballero, M. Barrejón, J. Cerdá, J. Aragó, S. Seetharaman, P. de la Cruz, E. Ortí, F. D'Souza and F. Langa, Self-Assembly-Directed Organization of a Fullerene–Bisporphyrin into Supramolecular Giant Donut Structures for Excited-State Charge Stabilization, *J. Am. Chem. Soc.*, 2021, **143**(29), 11199–11208.
34 C. J. Chancellor, F. L. Bowles, J. U. Franco, D. M. Pham, M. Rivera, E. A. Sarina, K. B. Ghiassi, A. L. Balch and M. M. Olmstead, Single-Crystal X-ray Diffraction Studies of Solvated Crystals of C60 Reveal the Intermolecular Interactions between the Component Molecules, *J. Phys. Chem. A.*, 2018, **122**(50), 9626–9636.
35 J. H. Deng, J. Luo, Y. L. Mao, S. Lai, Y. N. Gong, D. C. Zhong and T. B. Lu, π–π stacking interactions: Non-negligible forces for stabilizing porous supramolecular frameworks, *Sci. Adv.*, 2020, **6**(2), eaax9976.
36 J. Zhang, F. Bai, Y. Li, H. Hu, B. Liu, X. Zou, H. Yu, J. Huang, D. Pan, H. Ade and H. Yan, Intramolecular π-stacked perylene-diimide acceptors for non-fullerene organic solar cells, *J. Mater. Chem. A*, 2019, **7**(14), 8136–8143.
37 Z. Du, J. Xie, Y. Liu, Y. Tang, Q. Chen, X. Li and K. Zhu, A π-extended molecular belt with selective binding capability for fullerene C70, *Chem. Commun.*, 2024, **60**(50), 6387–6390.
38 C. Janiak, A critical account on π–π stacking in metal complexes with aromatic nitrogen-containing ligands, *J. Chem. Soc., Dalton Trans.*, 2000, **21**, 3885–3896.
39 P. Thordarson, Determining association constants from titration experiments in supramolecular chemistry, *Chem. Soc. Rev.*, 2011, **40**, 1305–1323.